Intense emission at 2.9 mu m from Yb3+/Ho3+ co-doped TeO2-Ga2O3-ZnO tellurite glasses

Yongqi Zhang, Xiaoxi Li, Weichao Wang, Xianghua Zhang, Yinsheng Xu

DR WEICHAO WANG (Orcid ID : 0000-0002-4597-3338)

DR YINSHENG XU (Orcid ID : 0000-0002-1887-0632)

Article type : Rapid Communication

Intense emission at 2.9 μm from Yb^{3+}/Ho^{3+} co-doped TeO_2–Ga_2O_3–ZnO tellurite glasses

Yongqi Zhang[1], Xiaoxi Li[1], Weichao Wang[2], Xianghua Zhang[1,3,*] Yinsheng Xu[1,2,*]

[1] *State Key Laboratory of Silicate Materials for Architectures, Wuhan University of Technology, Wuhan 430070, China*

[2] *State Key Laboratory of Luminescent Materials and Devices, Guangdong Provincial Key Laboratory of Fiber Laser Materials and Applied Techniques, South China University of Technology, Guangzhou 510640, China*

[3] *Laboratoire des Verres et Céramiques, UMR-CNRS 6226, Sciences chimiques de Rennes, Université de Rennes 1, Rennes, 35042, France*

Abstract:

Mid-infrared lasers have important applications in infrared countermeasures, sensing, environmental monitoring, biomedicine and many military and civilian fields. In this work, an intense emission at 2.9 μm from Yb^{3+}/Ho^{3+} co-doped TeO_2-Ga_2O_3-ZnO (TGZ) glass was reported. The 2 μm, 1.2 μm and visible emissions were also performed to understand the competitive luminescent mechanism. With the increase of Yb^{3+} ions concentration, all the emissions of Ho^{3+}

* Correspondence: Xianghua Zhang and Yinsheng Xu

Email: xzhang@univ-rennes1.fr (X. Z.), xuyinsheng@whut.edu.cn (Y. X.)

This article has been accepted for publication and undergone full peer review but has not been through the copyediting, typesetting, pagination and proofreading process, which may lead to differences between this version and the Version of Record. Please cite this article as doi: 10.1111/JACE.17766

increased while the emission of Yb^{3+} decreased due to the phonon-assisted energy transfer from Yb^{3+} ions to Ho^{3+} ions. The lifetimes of optimized 3 mol% Yb_2O_3 and 1 mol% Ho_2O_3 co-doped TGZ glass, which has the maximum emission intensity, are 548 μs and 1.7 ms at 2.9 and 2 μm, respectively. The Judd-Ofelt intensity parameters, absorption and emission cross-sections were calculated to evaluate the mid-infrared fluorescence properties of this new glass matrix material. The gain coefficients show that the 2.0 and 2.9 μm laser gain can be realized by small pump energy, indicating that this glass is a promising medium for the mid-infrared optical fiber laser.

Keywords: Tellurium glass; Yb^{3+}/Ho^{3+}; 2.9 μm; energy transfer

1. Introduction

Lasers with a wavelength of 2~3 μm have important application prospects in those civil and military fields such as laser medical surgery, atmospheric monitoring, remote sensing, due to the strong absorption in water and its eye-safe characteristic[1]. In this research, Ho^{3+} ion is a promising candidate for 2 and 2.9 μm lasers owing to the $^5I_7 \rightarrow {}^5I_8$ and $^5I_6 \rightarrow {}^5I_7$ transitions, respectively. However, it can not be obtained efficiently due to the lack of absorption bands matched with commercial 808 and/or 980 nm laser diodes (LDs). Therefore, sensitized excitation with rare-earth and/or semimetal co-doping such as Tm^{3+}/Ho^{3+}, Nd^{3+}/Ho^{3+}, Er^{3+}/Ho^{3+}, Bi^{3+}/Ho^{3+}, and other rare-earth co-doped glasses have attracted much attention as important matrix materials for 2~3 μm fiber lasers[2-5]. Moreover, Yb^{3+} has a relatively larger absorption cross-section at 980 nm, and there is a very effective energy transfer process between Yb^{3+} and Ho^{3+}, which perfectly solves the problem of Ho^{3+} lack of absorption band matching with commercial high-power LDs[6]. However, the current research on the Yb^{3+}/Ho^{3+} co-doped system mainly focuses on up-conversion and 2 μm emission. Although the introduction of Yb^{3+} can realize the population of electrons on the upper energy level of Ho^{3+}: 2.9 μm fluorescence (Ho^{3+}: $^5I_6$ energy level), few studies have considered the influence of Yb^{3+} incorporation on Ho^{3+}: 2.9 μm fluorescence because this emission is difficult to obtain due to the high non-radiative rate of $^5I_6$ level.

To achieve high efficient mid-infrared luminescence, the choice of glass matrix with low phonon energy and enough robust is very important, because non-radiative transitions can

significantly reduce the luminescence efficiency[1]. Based on the above requirements, the high-efficiency emission of Ho^{3+}: 2.9 μm fluorescence is mainly concentrated in fluoride glass and sulfide glass matrix, but their mechanical properties and chemical stability are poor[7]. Tellurite glass possesses relatively low phonon energy (~760 cm^{-1}) and a large transmission window[1, 8]. Meanwhile, it has better mechanical properties and chemical stability than fluoride and sulfide glasses. Nevertheless, in the field of mid-infrared fiber lasers, the ternary tellurite oxide glasses mainly conclude zinc sodium tellurite glass (TeO_2-ZnO-Na_2O), lanthanum tungsten tellurite glass (TeO_2-WO_3-La_2O_3), and barium lanthanum tellurite glass (TeO_2-BaO-La_2O_3), their low glass transition temperature and laser damage threshold limit the laser output power and further performance improvement[9]. In the previous work[10], it was found that TeO_2-Ga_2O_3-ZnO (TGZ) glass has low phonon energy (~760 cm^{-1}), excellent anti-devitrification properties (ΔT>100℃), high rare-earth-doping concentration, which is a new near- and mid-infrared laser glass matrix that can be expected to achieve 2.9 μm luminescence of Ho^{3+} ions.

In this work, Yb^{3+}/Ho^{3+} co-doped TGZ glasses were prepared by melt quenching technique. The absorption and luminescence properties of the prepared glasses were investigated in detail, especially the emission at 2.9 μm. The Judd-Ofelt (J-O) intensity parameters, absorption and emission cross-sections were calculated to evaluate the radiative and gain properties of the Ho^{3+}/Yb^{3+} co-doped TGZ glasses.

2. Experimental

2.1 Glass preparation

TGZ glasses with compositions of (84-*x*)TeO_2-5Ga_2O_3-10ZnO-*x*Yb_2O_3-1Ho_2O_3 (*x*=0.5, 1, 1.5, 2, 2.5, 3, in mol %) were prepared by a melt-quenching method. 10 g of raw materials were thoroughly mixed in an agate mortar. Then the batches were transferred into a muffle furnace and melted at 850 ℃ for 30 min. The melts were quenched onto a preheated copper plate for glass formation and the as-prepared glasses were annealed at 320 ℃ for 120 min in a muffle furnace. When the glass temperature drops to room temperature, the as-prepared glasses were cut and polished with a thickness of 1 mm for physical and spectroscopic measurements.

2.2 Measurements

The glass density was measured according to the Archimedes principle using a balance with kit for density determination. The de-ionized water was used as immersion liquid. The refractive index of the glass was measured by Metricon 2010-Type Prism coupler (test accuracy is ±0.001). Raman spectrum was conducted by Raman spectrometer (Renishaw in Via, Gloucestershire, UK) in the range of 200-1200 cm^{-1} with a 785 nm laser excitation. Absorption spectra were recorded by Perkin-Elmer Lambda 900 UV/VIS/NIR double beam spectrophotometer (Waltham, MA, US) with an error of ±1 nm. The emission spectra from visible to mid-infrared were collected by FLS980 fluorescence spectrometer, equipped with R928P PMT (for visible emissions), InGaAs detector (for 1~1.25 μm emission), and InSb detector (for 2~3 μm emission), respectively. The excitation source was 980 nm laser diode (LD). Fluorescence decay curves were recorded by a digital oscilloscope (TDS3012C, Tektronix) and signal generator (TDS3051C, Tektronix). All experiments were carried out at room temperature.

3. Results and discussion

3.1 Physical properties

As shown in Figure 1A, the transmittance of 3 mol% Yb_2O_3 and 1 mol% Ho_2O_3 co-doped TGZ glass reaches 72%, indicating this glass has good transparency. Inset shows no visible impurity particle inside the glass. The absorption bands will be analyzed in the following part. The refractive indices were fitted by Sellmeier dispersion equation, as shown in Figure 1B. With the increase of Yb^{3+} concentration, the density increased from 5.357 to 5.636 g/cm^3, as the inset of Figure 1B shown.

3.2 Absorption spectra and J-O theory analysis

The absorption spectra of Yb^{3+}/Ho^{3+} co-doped TGZ glasses in the range of 350-2500 nm were shown in Figure 2. Each assignment corresponding to the absorption transitions from the ground state to excited states of Ho^{3+} and Yb^{3+} ions were marked in the figure. The absorption bands of different samples showed the same intensity except for the band at 980 nm. The absorption band from Yb^{3+}: $^2F_{7/2}\rightarrow{}^2F_{5/2}$ near 980 nm (covering from $9.3\sim11.8\times10^3$ cm^{-1}) becomes stronger with the increase of Yb^{3+} concentration (the inset of Figure 2). The energy gap of Ho^{3+}: $^5I_8\rightarrow{}^5I_6$, which is close to the transition of Yb^{3+}: $^2F_{7/2}\rightarrow{}^2F_{5/2}$, can receive the electrons by

phonon-assisted energy transfer from Yb^{3+} ions.

The absorption spectra can be used to predict the spectroscopic parameters of rare-earth ions doped materials such as radiative transition probability, radiative lifetime, fluorescence branching ratio of various transitions through the Judd-Ofelt theory[11-14]. Using the J-O theory and the reduced matrix elements given in the literature[15], the J-O intensity parameters Ω_i (i=2, 4, 6) can be calculated. The density and refractive index used for calculation were 5.636 g/cm^3 and 1.965, respectively. Here the absorption bands at 1154, 644, 540, 454, and 418 nm of Ho^{3+}-doped TGZ glass were used to calculate the J-O intensity parameters, and the Ω_i (i=2, 4, 6) values of TGZ glass samples are 4.79, 3.43, and 1.31 ($\times10^{-20}$ cm^2), respectively. The root-mean-square error is 1.22×10^{-6}, indicating the results are reliable. Generally, J-O parameters can reflect the local environment information of rare-earth ions in the glass host, in which the value of Ω_2 mainly depends on the coordination field environment of rare-earth ions in the matrix, and as the symmetry around the rare-earth ions increases, the value of Ω_2 will be increased accordingly. Compared with the J-O strength parameters with Ho^{3+} ions in other matrices, Ω_2 of Yb^{3+}/Ho^{3+} co-doped TGZ glass in the present work show a larger value than that of fluoride glass (2.43×10^{-20} cm^2), phosphate glass (3.33×10^{-20} cm^2) and silicate glass (2.87×10^{-20} cm^2), but less than that of heavy metal lead-bismuth-gallium glass (5.15×10^{-20} cm^2). This may be related to the various polyhedrons that exist in the network of tellurite glass and the strong covalency degree between Ho^{3+} ions and ligand anions. The Ω_4/Ω_6 value indicates favorable mid-infrared emission. The TGZ glass with a relatively higher Ω_4/Ω_6 value indicates good mid-infrared emission quality.

Based on the J-O intensity parameters, the electric dipole transition probability (A_{ed}), the magnetic dipole transition probability (A_{md}), the spontaneous emission transition probability (A_{rad}), the fluorescence branch ratio (β) and radiation lifetime (τ_{rad}) are listed in Table 2. It can be seen that the τ_{rad} of the Ho^{3+}: $^5I_6$ energy level (2948 μs) is less than that of the Ho^{3+}: $^5I_7$ lower energy level (5704 μs), indicating the $^5I_6\rightarrow{}^5I_7$ transition is a typical self-terminating process. Additionally, as listed in Table 2, the A_{rad} of the Ho^{3+}: $^5I_6\rightarrow{}^5I_7$ transition is 55.02 s^{-1}, which is larger than that of fluoride (31.43 s^{-1}), phosphate (19.21 s^{-1}), fluorophosphate (34.11 s^{-1}) and lanthanum-tungsten-tellurite (41.2 s^{-1}) glass, but smaller than that of chalcogenide glass (113 s^{-1})[20].

The relatively bigger A_{rad} would provide a higher probability to achieve mid-infrared laser action at 2.9 μm in this TGZ glass.

3.4 Mid-infrared and up-conversion luminescence analysis

Under the excitation at 980 nm, the emissions from visible to mid-infrared can be collected by different detectors. Figure 3 shows the 2.9 μm, 1-1.25 μm, 2.0 μm and visible emission spectra of Yb^{3+}/Ho^{3+} co-doped TGZ glass samples with different concentrations of Yb^{3+}. When the phonon-assisted energy transfer from Yb^{3+} to Ho^{3+} occurred, the $^5I_6$ level was populated and then the electrons fall to the lower $^5I_7$ level and ground state radiatively. In this way, 2.9 μm and 1.2 μm emissions can be seen as shown in Figures 3A and 3B, corresponding to the transitions of Ho^{3+}: $^5I_6 \rightarrow {}^5I_7$ and Ho^{3+}: $^5I_6 \rightarrow {}^5I_8$, respectively. With the increase of the Yb_2O_3 concentration from 0.5 to 3 mol%, the 2.9 and 1.2 μm emissions increased 2.9 and 2.3 times, respectively. For emission at 2.9 μm, only one main peak centered at 2851 nm with the full width at half maximum (FWHM) of 70 nm. For emission at 1.2 μm, two peaks centered at 1155 and 1186 nm can be identified by Gaussian fitting due to the Stark energy level splitting. The emission at 1.06 μm (Yb^{3+}: $^2F_{5/2} \rightarrow {}^2F_{7/2}$) decreased around 2 times, indicating the energy transfer process from Yb^{3+} to Ho^{3+} becomes more efficient. The small overlap between the 1100 nm and 1155 nm emissions evidenced that the ET occurs from Yb^{3+} to Ho^{3+} ions.

Besides, partial electrons can non-radiatively transit to the $^5I_7$ level and then fall to the ground state and emit 2.0 μm photons. As shown in Figure 3C, the 2 μm emission covering from 1850 to 2200 nm increased 3.2 times with the increase of the Yb^{3+} concentration. The FWHM of this emission is 150 nm and the deconvolution shows two emission bands peaked at 1957 nm and 2045 nm.

To understand the luminescence mechanism, the up-conversion emission from 450 nm to 750 nm was also recorded. As shown in Figure 3D, two visible up-conversion emission bands are located at 543 nm ($^5S_2$, $^5F_4 \rightarrow {}^5I_8$) and 656 nm ($^5F_5 \rightarrow {}^5I_8$) can be observed, respectively. The intensity of these two up-conversion emissions increased more than 7 times with the increase of Yb^{3+} ions concentration. In contrast, the luminous intensity of visible band increased more than that of the infrared band. The detailed mechanism will be explained with the energy diagram.

From the above results, all the emissions of Ho^{3+} increased with the increase of Yb^{3+} concentration, while emission of Yb^{3+} decreased gradually. This is mainly attributed to the following two aspects: (1) The high contents of Yb_2O_3 in the TGZ glasses promote the energy transfer between Yb^{3+} and Ho^{3+}, so the number of particles on the $^5I_6$ and $^5I_7$ energy levels of Ho^{3+} is greatly increased to enhance the corresponding luminescence. (2) The structural units in the present glasses include [TeO_4] trigonal bipyramids, [TeO_{3+1}] polyhedra and [TeO_3] triangular pyramids. The low phonon energy of [TeO_4] trigonal bipyramids in the TGZ glass (~760 cm^{-1}) effectively reduces the multiphonon relaxation rate of the sample[10], thus contributing to the enhancement of the radiation transition process in the mid-infrared range.

3.5 Energy level lifetime analysis

The fluorescence decay curves of Ho^{3+}/Yb^{3+} co-doped TGZ glass samples with different doping contents under excitation at 980 nm were recorded as shown in Figure 4. The lifetime at 2 μm can be fitted by a single exponential equation very well, hence we can easily determine the lifetime when the intensity decreased to e^{-1}. As can be seen from Figure 4A, the fluorescence lifetime of 2 μm of the glass samples decreased a little from 2 ms to 1.7 ms. This is because the energy transfer from Yb^{3+} to Ho^{3+} mainly occurs at the $^5I_6$ energy level, so the particle distribution of the $^5I_7$ energy level is slightly affected. Therefore, with the increase of Yb^{3+} concentration, the $^5I_7$ level lifetime of Ho^{3+} does not change significantly.

Both the 2.9 and 1.2 μm emissions are from the $^5I_6$ level, so the decay lifetime of $^5I_6$ level by monitoring at 2.9 μm were measured. The decay curves are composed of a fast decay and a slow decay which can be fitted by a double exponential equation. As the inset table listed in Figure 4B, the average lifetimes of 2.9 μm emission increased from 272 to 548 μs, the quantum efficiency ($\eta=\tau_e/\tau_{rad}$) increased from 9.2% to 18.5%, correspondingly. With the increase of Yb^{3+} concentration, the energy transfer process from Yb^{3+} to Ho^{3+} becomes more efficient, resulting in a longer lifetime of $^5I_6$ energy level of Ho^{3+}. On the other hand, it can be seen that the experimental lifetime of the $^5I_6$ level is much shorter than that of the $^5I_7$ level, which may be related to the strong non-radiative relaxation of the $^5I_6$ level in the tellurite glass. Meanwhile, as shown in Figure 4C, the fluorescence lifetime of 1.06 μm of the glass samples decreased from 460

μs to 280 μs, indicating high concentration of Yb^{3+} is beneficial to improve the energy transfer efficiency.

3.6 Evaluation of the laser gain properties

The absorption and emission cross-sections are important criteria for evaluating the quality of laser gain materials. The emission cross-sections (σ_e) at 2 and 2.9 μm from TGZ glass with 3 mol% Yb_2O_3 and 1mol% Ho_2O_3 are subsequently calculated using the calculation equation of absorption cross-section (σ_a) and F-L theory[14] according to the absorption and emission spectra. Since the absorption of Ho^{3+}: $^5I_7 \rightarrow {}^5I_6$ belongs to the excited state absorption, it is difficult to measure the precise spectrum pattern of its absorption spectrum, so the McCumber theory was used to determine it. Among them, the value of the parameter E_0 can be determined by the position of the fluorescence peak of the Ho^{3+}: $^5I_6 \rightarrow {}^5I_7$ transition in the emission spectrum. Besides, due to the lack of accurate electronic structure information of Ho^{3+}, it is assumed that the $^5I_6$ and $^5I_7$ energy levels are split into 13 and 15 sub-levels using the simplified model proposed by Quimby[21], respectively, and the sub-levels are uniformly distributed in each manifold. From this, it can be estimated that the Z_l/Z_u value of the Ho^{3+}: $^5I_6 \rightarrow {}^5I_7$ transition process is about 1.12.

As shown in Figure 5, the σ_a and σ_e of the transitions were calculated. The σ_a of $^5I_8 \rightarrow {}^5I_7$ transition of Ho^{3+} is located at 1952 nm with a maximum value of 0.57×10^{-20} cm^2 and a FWHM of 104 nm, while the σ_e of $^5I_7 \rightarrow {}^5I_8$ transition is located at 2052 nm with a maximum value of 0.73×10^{-20} cm^2 and a FWHM of 123 nm. Similarly, the σ_e of $^5I_6 \rightarrow {}^5I_7$ transition of Ho^{3+} is located at 2854 nm with a maximum value of 1.28×10^{-20} cm^2, which is higher than that of ZBLAN glass (0.50×10^{-20} cm^2)[22], germanate glass (0.92×10^{-20} cm^2)[23], fluoride glass (0.98×10^{-20} cm^2)[24], but smaller than that of fluoroaluminate glass (1.91×10^{-20} cm^2)[25]. According to the McCumber theory, the σ_e of $^5I_6 \rightarrow {}^5I_7$ transition is located at 2849 nm with a maximum value of 1.15×10^{-20} cm^2.

Based on the absorption and emission cross-sections, the gain coefficient spectra of Ho^{3+}: $^5I_7 \rightarrow {}^5I_8$ and $^5I_6 \rightarrow {}^5I_7$ transitions in Ho^{3+}/Yb^{3+} co-doped TGZ glass sample can be obtained by using the formula from Ref. 14. As shown in Figure 6, The p value representing the electron population ratio between the two energy levels gradually changes from 0 to 1. It can be seen from Figure 6A that a positive gain can be obtained when $p \geq 0.2$, indicating that TGZ glass has potential

application prospects as a matrix material for 2 μm fiber laser. As shown in Figure 6B, the same formula can be used to obtain the gain coefficient spectra at 2.9 μm. It can be seen that a positive gain can be obtained when $p \geq 0.4$, which indicates that theoretically, a 2.9 μm laser pulse can be obtained in the TGZ glass with smaller pump energy.

3.7 Energy transfer mechanism

Figure 7 illustrates the energy levels of the Yb^{3+}/Ho^{3+} co-doped system. Based on the emission spectra of this study and previous related studies, the possible energy transfer process is marked. Under the excitation of 980 nm LD, Yb^{3+} absorbs 980 nm photons and the electrons were excited from the ground state $^2F_{7/2}$ energy level to the excited state $^2F_{5/2}$ energy level. With the participation of phonons, Yb^{3+} can transfer energy to Ho^{3+} through the energy transfer process of Yb^{3+}: $^2F_{5/2}$+Ho^{3+}: $^5I_8 \rightarrow Yb^{3+}$: $^2F_{5/2}$+Ho^{3+}: $^5I_6$, so that the $^5I_6$ energy level was populated. Meanwhile, with the increase of Yb^{3+} doping concentration, the strong absorption of $^2F_{7/2} \rightarrow ^2F_{5/2}$ promotes the population of electrons at the $^5I_6$ energy level. The electrons at the Ho^{3+}: $^5I_6$ energy level have three paths to relax. First, some of these electrons are radiated back to the ground state and emits near-infrared fluorescence of 1.2 μm. Second, partial electrons can relax to the $^5I_7$ level radiatively and yield 2.9 μm emission. Third, the remaining electrons fall back to the ground state non-radiatively. The electrons on $^5I_7$ level can relax to the $^5I_8$ level radiatively and yield 2 μm emission.

The strong visible emissions at 543 nm and 656 nm (as shown in Figure 3D,) are mainly because the electrons at the $^5I_6$ and $^5I_7$ energy levels are excited to the $^5S_2$, $^5F_4$ and $^5F_5$ states through the excited state absorption (ESA) and the energy transfer (ET) processes between Yb^{3+} and Ho^{3+} ions[26]. The electrons at the $^5S_2$, $^5F_4$ excited state emit 543 nm green fluorescence through the $^5S_2$, $^5F_4 \rightarrow ^5I_8$ radiation transition. Small part of electrons at the $^5F_4$ state fall to the $^5F_5$ energy level through the multiphonon relaxation process. The $^5F_5$ energy level can also be populated by the energy transfer process, and then the electrons radiatively fall back to the ground state and emit 656 nm red light.

4. Conclusions

The Ho^{3+}/Yb^{3+} co-doped TeO_2–Ga_2O_3–ZnO glasses were prepared for the investigation of the

2.9 μm luminescent properties. The J-O intensity parameters, spontaneous emission probability, fluorescence branch ratio and radiation lifetime of the 3 mol% Yb_2O_3 and 1 mol% Ho_2O_3 co-doped TGZ glass samples were calculated. The luminescence characteristics from visible to mid-infrared ranges of the Ho^{3+}/Yb^{3+} co-doped TGZ glass under 980 nm LD excitation were studied. With the increase of Yb^{3+} doping concentration, the emission of Ho^{3+} at 1.2 μm, 2 μm and 2.9 μm increased while the emission of Yb^{3+} at 1.06 μm decreased. Besides, the fluorescence lifetime of 2.9 μm increased from 272 to 548 μs with the increase of Yb^{3+} doping concentration, while the fluorescence lifetime of 2 μm decreased a little from 2 ms to 1.7 ms. The emission and absorption cross-sections and corresponding gain coefficients of Ho^{3+}: $^5I_7 \rightarrow {}^5I_8$ and $^5I_6 \rightarrow {}^5I_7$ transitions in the present glass indicate that the TGZ glass is a good laser gain medium for 2.0 and 2.9 μm fiber lasers. The results show that this glass has potential applications for mid-infrared fiber amplifiers and laser devices.

Acknowledgements

This work is financially jointly supported by the National Natural Science Foundation of China (61975156), Fundamental Research Funds for the Central Universities (203134001), Hubei Natural Science Foundation (2020CFB641), Open Fund of the State Key Laboratory of Luminescent Materials and Devices (South China University of Technology), and Open Fund of the Guangdong Provincial Key Laboratory of Fiber Laser Materials and Applied Techniques (South China University of Technology).

References

1. Jha A, Richards B, Jose G, et al. Rare-earth ion doped TeO_2 and GeO_2 glasses as laser materials. *Prog. Mater Sci.* 2012;57(8):1426-1491.
2. Shin YB, Lim HT, Choi YG, Kim YS, Heo J. 2.0 μm emission properties and energy transfer between Ho^{3+} and Tm^{3+} in PbO-Bi_2O_3-Ga_2O_3 glasses. *J. Am. Ceram. Soc.* 2000;83(4):787-791.
3. Chen R, Tian Y, Li B, et al. Efficient 2 μm emission in Nd^{3+}/Ho^{3+} co-doped silicate-germanate glass pumped by common 808 nm LD. *Opt. Laser Technol.* 2017;89:108-113.
4. Kang S, Yu H, Ouyang T, et al. Novel Er^{3+}/Ho^{3+}-codoped glass-ceramic fibers for broadband tunable mid-infrared fiber lasers. *J. Am. Ceram. Soc.* 2018;101(9):3956-3967.

5. Cao W, Wang T, Huang F, et al. Tuning the micro-structure of germanosilicate glass to control Bi^0/Bi^+ and promote efficient Ho^{3+} fluorescence. *Dalton Trans.* 2018;47(29):9717-9723.
6. Balaji S, Gupta G, Biswas K, Ghosh D, Annapurna K. Role of Yb^{3+} ions on enhanced ~2.9 μm emission from Ho^{3+} ions in low phonon oxide glass system. *Sci. Rep.* 2016;6:29203.
7. Hou G, Zhang C, Fu W, Li G, Xia J, Ping Y. Broadband mid-infrared 2.0 μm and 4.1 μm emission in Ho^{3+}/Yb^{3+} co-doped tellurite-germanate glasses. *J. Lumin.* 2020;217:116769.
8. Wang WC, Zhou B, Xu SH, Yang ZM, Zhang QY. Recent advances in soft optical glass fiber and fiber lasers. *Prog. Mater Sci.* 2019;101:90-171.
9. Gupta G, Balaji S, Biswas K, Annapurna K. Enhanced luminescence at 2.88 and 2.04 μm from Ho^{3+}/Yb^{3+} codoped low phonon energy TeO_2–TiO_2–La_2O_3 glass. *AIP Adv.* 2019;9(4):045201.
10. Mao LY, Liu JL, Li LX, Wang WC. TeO_2-Ga_2O_3-ZnO ternary tellurite glass doped with Tm^{3+} and Ho^{3+} for 2 μm fiber lasers. *J. Non-Cryst. Solids* 2020;531:119855.
11. Judd BR. Optical absorption intensities of rare-earth ions. *Phys. Rev.* 1962;127:750-761.
12. Ofelt GS. Intensities of crystal spectra of rare-earth Ions. *J. Chem. Phys.* 1962;37(3):511-520.
13. Librantz AFH, Jackson SD, Gomes L, Ribeiro SJL, Messaddeq Y. Pump excited state absorption in holmium-doped fluoride glass. *J. Appl. Phys.* 2008;103(2):023105.
14. Huang F, Liu X, Hu L, Chen D. Optical properties and energy transfer processes of Ho^{3+}/Er^{3+}-codoped fluorotellurite glass under 1550 nm excitation for 2.0 μm applications. *J. Appl. Phys.* 2014;116(3):033106.
15. Rukmini E, Jayasankar CK. Spectroscopic properties of Ho^{3+} ions in zinc borosulphate glasses and comparative energy level analyses of Ho^{3+} ions in various glasses. *Opt. Mater.* 1995;4:524-546.
16. Kim JW, Mackenzie JI, Parisi D, Veronesi S, Tonelli M, Clarkson WA. Efficient in-band pumped Ho: $LuLiF_4$ 2 μm laser. *Opt. Lett.* 2010;35(3):420-422.
17. Tian Y, Zhang LY, Xu RR, Hu LL, Zhang JJ. 2 μm emission properties in Tm^{3+}/Ho^{3+} codoped fluorophosphate glasses. *Appl. Phys. B* 2010;101(4):861-867.
18. Bai G, Guo Y, Tian Y, Hu L, Zhang J. Light emission at 2 μm from Ho-Tm-Yb doped silicate glasses. *Opt. Mater.* 2011;33(8):1316-1319.

19. Chen BJ, Shen LF, Pun EYB, Lin H. ~1.2 μm near-infrared emission and gain anticipation in Ho^{3+} doped heavy-metal gallate glasses. *Opt. Commun.* 2011;284:5705-5709.
20. Huang B, Xu C, Zhang Z, Zang Cy, Sun L. Removal of hydroxyl routes enhancing 2.85 μm mid-infrared luminescence in oxyfluorotellurite glass with high ZnF_2 content. *J. Non-Cryst. Solids* 2018;502:97-105.
21. Digonnet MJF, Murphy-Chutorian E, Falquier DG. Fundamental limitations of the McCumber relation applied to Er-doped silica and other amorphous-host lasers. *IEEE J. Quantum Electron.* 2002;38(12):1629-1637.
22. Li J, Gomes L, Jackson SD. Numerical modeling of holmium-doped fluoride fiber lasers. *IEEE J. Quantum Electron.* 2012;48(5):596-607.
23. Cai M, Zhou B, Tian Y, Zhou J, Xu S, Zhang J. Broadband mid-infrared 2.8 μm emission in Ho^{3+}/Yb^{3+}-codoped germanate glasses. *J. Lumin.* 2016;171:143-148.
24. Huang F, Liu X, Zhang Y, Hu L, Chen D. Enhanced 2.7- and 2.84-μm emissions from diode-pumped Ho^{3+}/Er^{3+}-doped fluoride glass. *Opt. Lett.* 2014;39(20):5917-5920.
25. Zhou B, Wei T, Cai M, et al. Analysis on energy transfer process of Ho^{3+} doped fluoroaluminate glass sensitized by Yb^{3+} for mid-infrared 2.85 μm emission. *J. Quant. Spectrosc. Radiat. Transfer* 2014;149:41-50.
26. Rakov N, Maciel GS, de Araújo CB, Messaddeq Y. Energy transfer assisted frequency upconversion in Ho^{3+} doped fluoroindate glass. *J. Appl. Phys.* 2002;91(3):1272-1276.

Table List

Table 1 J-O parameters Ω_i (i=2, 4, 6) of Ho^{3+} ions in TGZ glasses

Table 2 Calculated transition probabilities of the electric dipole (A_{ed}), magnetic dipole (A_{md}), total spontaneous radiative probabilities (A_{rad}), branching ratios (β), and radiative lifetimes (τ_{rad}) of Yb^{3+}/Ho^{3+} co-doped TGZ glass.

Table 1

Matrix	Ω_i ($\times 10^{-20}$ cm^2)			Ω_4/Ω_6	Ref.
	Ω_2	Ω_4	Ω_6		
fluoride glass	2.43	1.67	1.84	0.91	[16]
phosphate glass	3.33	3.01	0.61	4.93	[17]

silicate glass	2.87	1.71	0.69	2.48	[18]
lead-bismuth-gallium glass	5.15	2.79	2.29	1.22	[19]
gallium zinc tellurite glass	4.79	3.43	1.31	2.62	This work

Table 2

Initial state	Final state	A_{ed} (s^{-1})	A_{md} (s^{-1})	A_{rad} (s^{-1})	β (%)	τ_{rad} (μs)
$^5I_7$	$^5I_8$	127.35	47.96	175.31	100	5704
$^5I_6$	$^5I_8$	284.22	—	284.22	84	—
	$^5I_7$	30.80	24.22	55.02	16	2948
$^5I_5$	$^5I_8$	109.96	—	109.96	40	—
	$^5I_7$	140.28	—	140.28	50	—
	$^5I_6$	14.61	13.49	28.10	10	3593
$^5F_5$	$^5I_8$	4022.27	—	4022.27	77	
	$^5I_7$	992.72	—	992.72	19	
	$^5I_6$	190.92	—	190.92	4	
	$^5I_5$	14.40	—	14.40	0	192
$^5F_4$	$^5I_8$	6615.40	—	6615.40	76	
	$^5I_7$	1010.41	—	1010.41	12	
	$^5I_6$	644.55	—	644.55	7	
	$^5I_5$	246.26	—	246.26	3	
	$^5F_5$	107.56	42.13	149.69	2	119
$^5F_3$	$^5I_8$	3050.99	—	3050.99	40	
	$^5I_7$	3258.90	—	3258.90	42	
	$^5I_6$	796.03	—	796.03	10	
	$^5I_5$	501.23	—	501.23	7	
	$^5F_5$	56.74	—	56.74	1	

	$^5F_4$	4.31	4.42	8.73	0	130

Figure Captions

Figure 1 A, Transmission spectrum of 3 mol% Yb_2O_3 and 1 mol% Ho_2O_3 co-doped TGZ glass. Inset is the photo of glass sample (size: 17 mm×12 mm×1 mm). B, Dispersion curves (scatter points represent the measured refractive indices and the curves were fitted by Sellmeier dispersion formula) and density (inset) of TGZ glasses

Figure 2 Absorption coefficient of Yb^{3+}/Ho^{3+} co-doped TGZ glasses. Inset is the integrated area of the absorption bands at 980 nm with the increase of Yb_2O_3 concentration

Figure 3 Emission spectra of TGZ glass samples with 1 mol% Ho_2O_3 and different Yb^{3+} contents excited by 980 nm LD monitoring at A: 2.9 μm, B: 1-1.25 μm, C: 2 μm, and D: visible emissions, respectively. The grey solid lines in figure B and C are the deconvolution of emission spectrum of 3 mol% Yb_2O_3 and 1 mol% Ho_2O_3 co-doped TGZ glass

Figure 4 Decay curves of Ho^{3+}/Yb^{3+} co-doped TGZ glass samples monitoring at A: 2 μm, B: 2.9 μm and C: 1.06 μm emissions upon the excitation of 980 nm LD

Figure 5 Absorption and emission cross-sections of Ho^{3+}/Yb^{3+} co-doped TGZ glass at 2 and 2.9 μm, respectively

Figure 6 Calculated gain coefficients corresponding to the A: $^5I_8 \leftrightarrow {}^5I_7$ and B: $^5I_7 \leftrightarrow {}^5I_6$ transitions of 3 mol% Yb_2O_3 and 1 mol% Ho_2O_3 co-doped TGZ glass

Figure 7 Energy level diagram and energy transfer mechanism of Yb^{3+}/Ho^{3+} co-doped system

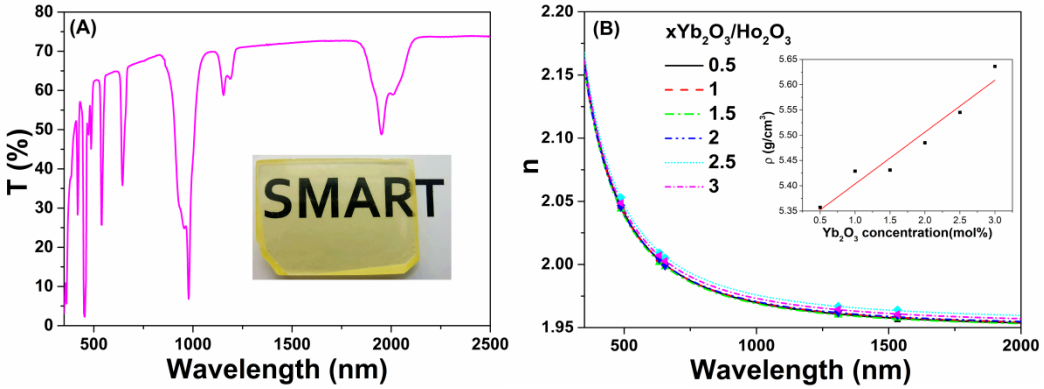

jace_17766_f1.tif

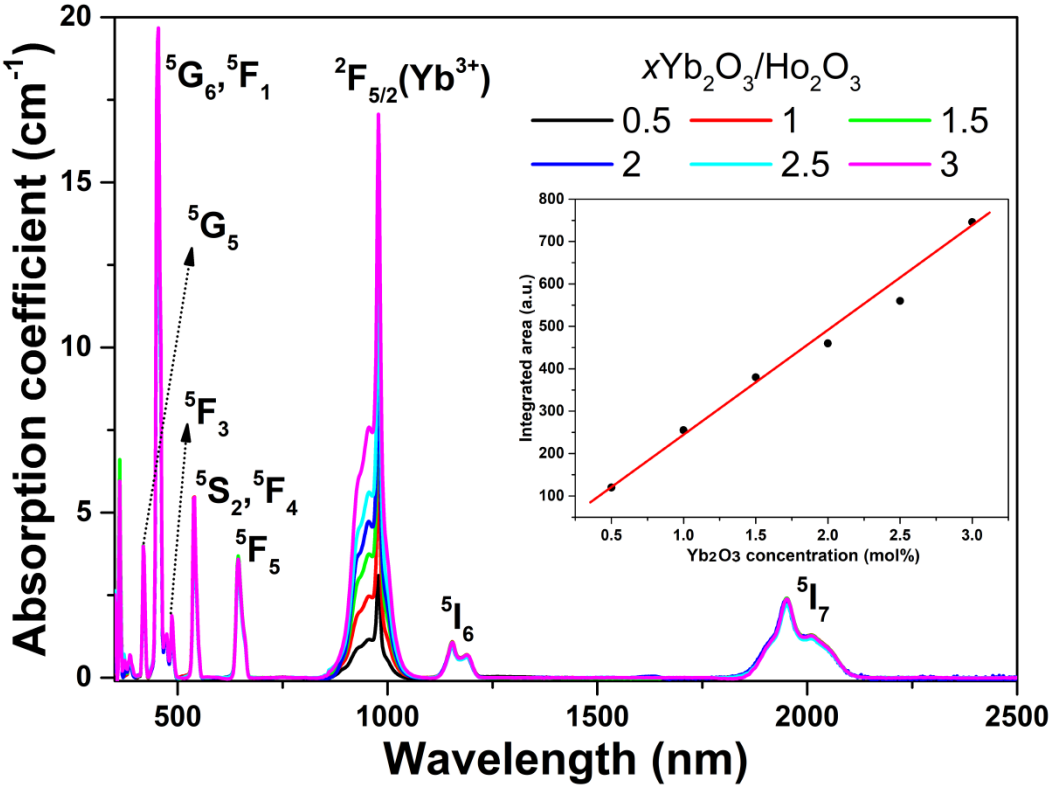

jace_17766_f2.tif

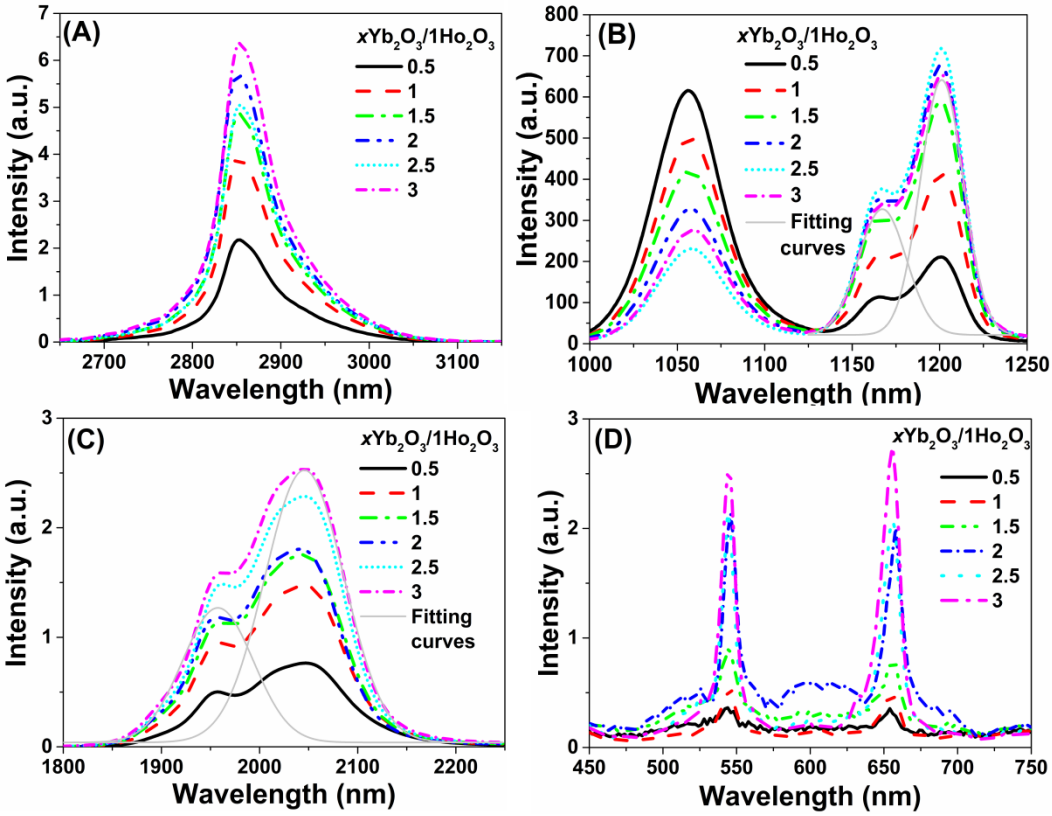

jace_17766_f3.tif

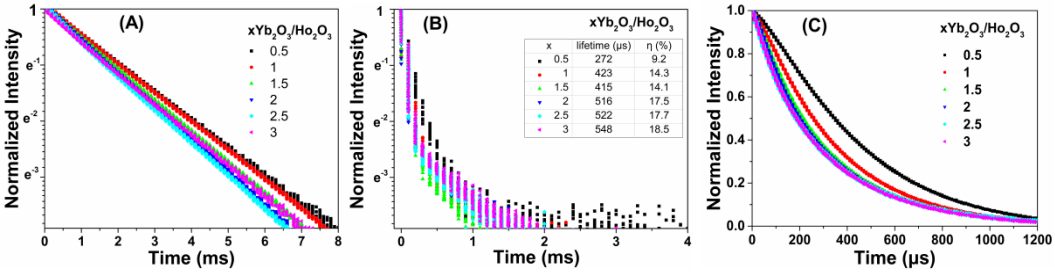

jace_17766_f4.tif

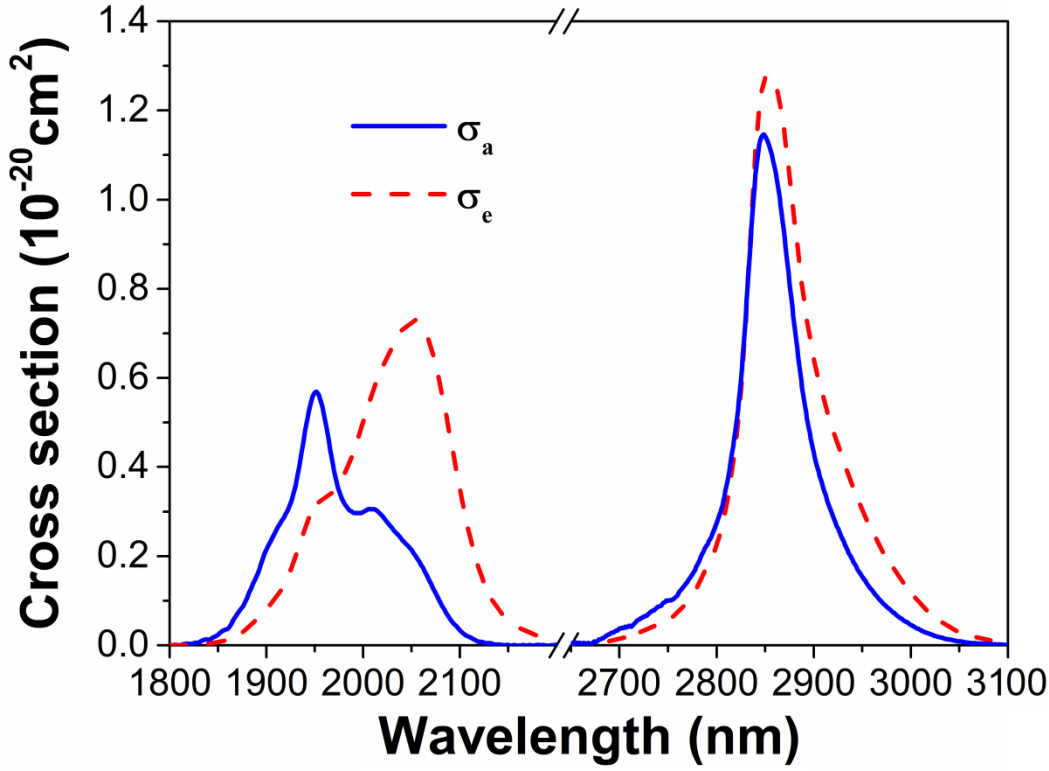

jace_17766_f5.tif

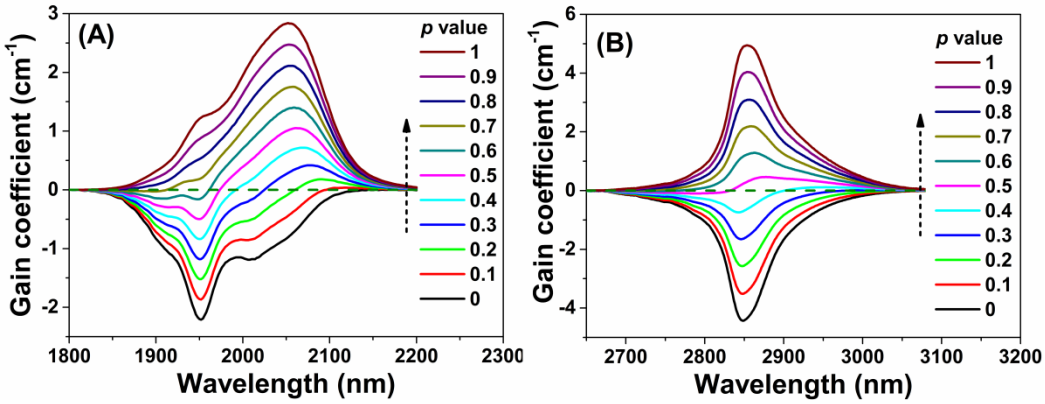

jace_17766_f6.tif

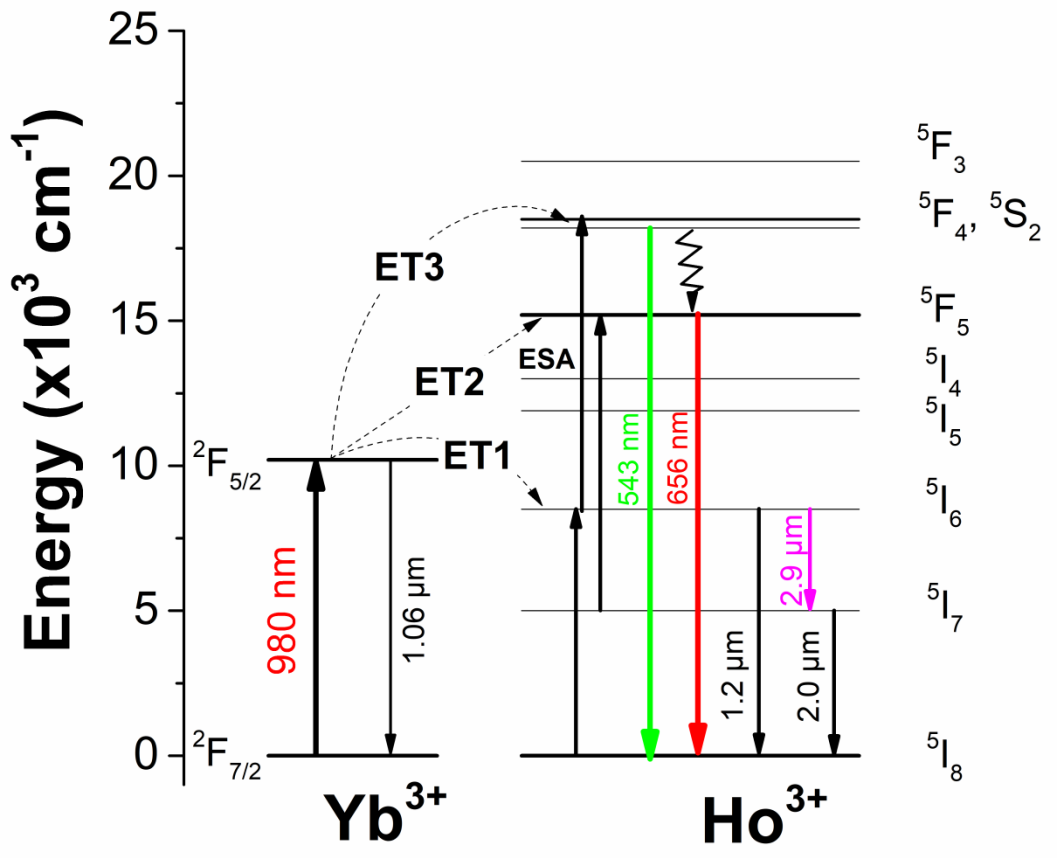

jace_17766_f7.tif